14th Australasian Fluid Mechanics Conference
Adelaide University, Adelaide, Australia
10-14 December 2001

Particle-Pair Separation Processes in Turbulence

M.S. Borgas[1] and P.K. Yeung[2]

[1]CSIRO Atmospheric Research
Aspendale, Victoria, 3195. AUSTRALIA

[2]School of Aerospace Engineering
Georgia Institute of Technology, Georgia, 30332. USA.

Abstract

The role of viscous effects during the Lagrangian separation process for pairs of fluid particles moving apart in turbulent flow is highlighted. New models based on the important physics are compared with direct numerical simulations. Rare but extreme flow events (large strains) are identified and are shown to critically constrain the model separation performance. Adequate account of the extremes is essential for good models, but has not been adopted previously in the literature.

Introduction

The separation with time of initially close particle pairs in natural turbulence (say of the atmosphere and ocean) is an important process and, for example, determines concentration fluctuations in pollution plumes, droplet interactions in clouds, swimming predator-prey plankton encounters, amongst other phenomena. The separation problem is simply the task of accurately modelling the speed and statistics of random separations as functions of time, which has proven to be a difficult task even after eighty or so years of effort following on from Lewis Fry Richardson in 1926 [1], recently summarised in [2]. The classic Lagrangian inertial-range law has a coefficient with at least an order of magnitude of uncertainty: the mean-square separation grows like the product of the cube of elapsed time, the turbulent kinetic energy dissipation rate, and an uncertain numerical coefficient between 0.01 and 2. However, for many close particle-particle interactions, the important physical processes are those controlled by viscous effects. This note focuses on those effects and their representation with simple models, as a step to modelling all scales in turbulent separation problems. We propose a stochastic differential equation as the model for instantaneous Lagrangian acceleration, despite recent criticisms of this assumption. The importance of fast accelerations and maximum "strain-rates" is demonstrated, and the extreme-value nature of the important processes explains the earlier difficulty in achieving good results. Comparisons with Lagrangian results from direct numerical simulations of turbulent flow demonstrate that a well-posed model performs remarkably well.

Pair Separation Models

Pairs of distinct fluid particles can be characterised by the magnitude of the distance, l, between them. Often questions of practical significance depend on the behaviour of l with time. For example, for populations of plankton in the ocean with a given initial encounter separation l_0, at later times what proportion stay in contact (say with $l \le l_0$) under turbulent advection? Or for an emission from a small chimney in the atmosphere, of radius l_0 say, the issue is how long before average local dilutions, reflected by growing root-mean-square values of the meandering plume width l, render the local plume concentrations "safe."

Many models for the random growth of l exist (see [2]), generally for ideal homogeneous and isotropic turbulence. Because the separation process of interest is inherently small scale, such idealisation is well justified. Direct numerical simulations of (ideal) turbulence [3] also describe detailed properties for l, highlighting extreme behaviour for particle pairs with very small initial separations. For this case a tiny number of particles rapidly separate, but many remain close together, causing the statistical properties like the skewness and the flatness factor to be anomalously large and very hard to predict with simple models.

Basic diffusion processes do not generally describe highly non-Gaussian separation behaviour, and more advanced models are necessary. One of the simplest such models for representing the separation process is a stochastic differential equation for the separation rate, $u = dl/dt$,

$$du = a(u,l)dt + \chi(l)dW, \quad dl = udt \tag{1}$$

where dW is random white noise [4], with the properties that $\overline{dW} = 0$ and $\overline{dW^2} = dt$, where the overbar indicates a mean quantity. The function $a(u,l)$ in (1) is chosen to accurately reflect Eulerian velocity-field properties [5,6] and the function $\chi(l)$ depends on viscous properties for small separations [7]. However, previous applications of (1) to relative dispersion have not successfully captured the extreme variability of the viscous separation process [7], and better performance of alternative models [8] has led to concerns of the general applicability of stochastic models like (1). This is despite the widespread success such models achieve for turbulent dispersion, particularly in atmospheric pollution problems [9,10].

However, the careful analysis in this note will demonstrate that model (1) is fully adequate when appropriate detail is incorporated in the formulation, in particular when all the relevant Eulerian information is encoded into the model. This information is embodied in the probability density function (pdf) for the velocity increment u at fixed separation l: $P_E(u;l)$. Most models in the literature effectively represent this pdf with Gaussian tails, i.e. $P_E(u;l) \sim \exp\left(-\tfrac{1}{2}u^2/\sigma_\pm^2\right)$ as $u \to \pm\infty$. In general this means that the drift term a in (1) is too small at large u to rapidly accelerate separation velocities to large amplitude and consequently the separation itself to large values. We find instead that it is necessary to represent the pdf tails with power-law ranges, $P_E(u;l) \sim |u|^{-\phi}$ for sufficiently large $|u|$ (but not strictly as $u \to \pm\infty$), to get separation behaviour that corresponds with observations [3, 8]. To clearly demonstrate these critical properties, which are essential for complete modelling of separation processes in turbulent dispersion, it is sufficient in the first instance to consider separation processes

solely in the dissipation sub-range. There, all processes are viscosity dependent, and the flow varies "smoothly" (analytically) in space, and the separation velocities are completely characterised by random straining fields. The key pdf is now the Eulerian pdf for the strain, *s*, but this is simply obtained from $P_E(u;l)$ in the limit as $l \to 0$.

Dissipation Sub-Range Separation Processes

The process now considered is when initial separations are so small that viscous effects always dominate. The turbulent flow at small scales is defined statistically, as usual, by the key parameters of the mean energy dissipation rate per unit mass $\bar{\varepsilon}$ and the kinematic viscosity ν. Thus a length scale for viscous effects is just Kolmogorov's microscale, $\eta = (\nu^3/\bar{\varepsilon})^{1/4}$, and a time scale is $t_\eta = (\nu/\bar{\varepsilon})^{1/2}$, both standard quantities [11]. Of course, for the atmosphere or ocean, these are tiny scales, but the purpose here is to compare models with numerical simulations, which currently have only modest separations of scale. The process we consider is the separation in time of particle pairs with initial separations $l_0 << \eta$, but for finite times $t >> t_\eta$ with the restriction that $l(t) << \eta$. Note that eventually nearly all particle pairs will separate beyond the viscous scales, but for pairs sufficiently close together initially, the length of time that particles stay together can be indefinite. In practice, when $l \le 4\eta$ dissipation sub-range approximations suffice. These restrictions mean that the velocity increment over a fixed separation *l* is proportional to the distance *l* multiplied by the local strain-rate *s*: $u = sl$. The Eulerian statistics for these variables are the usual longitudinal variables, i.e. for cartesian coordinates

$$u = (u_i(\underline{x}+\underline{l}) - u_i(\underline{x}))l_i/l, \quad s = \frac{\partial u_1}{\partial x_1} \quad (l^2 = l_i l_i). \tag{2}$$

Eulerian properties for both these variables are well known [11]: the *Eulerian* averages $\overline{s^2} = \sigma_s^2$ and $\overline{u_1^2} = \sigma_u^2$ define a convenient Reynolds number, the Taylor-scale Reynolds number, as $\mathrm{Re}_\lambda = \sigma_u^2/\nu\sigma_s$. For atmospheric flows we can have $\mathrm{Re}_\lambda > 10^3$, but for numerical simulations the state-of-the-art is $\mathrm{Re}_\lambda \sim 230$ [13]. The identity $\bar{\varepsilon} = \frac{1}{15}\sigma_s^2/\nu$ should also be noted.

The stochastic model in the dissipation sub-range is simply derived from (1) by noting that all two-point increment variables must be proportional to *l*; thus $u = sl$, $a = \omega(s)l$, $\chi = \chi_0 l$ and $du = dsl + sdl = dsl + s^2 ldt$. Taken together, the stochastic model for the joint evolution of the strain rate and the separation decouples in the dissipation sub-range and is modelled by the pair of equations

$$ds = (\omega(s) - s^2)dt + \chi_0 dW, \quad l = l_0 \exp\left(\int_0 s(t')dt'\right). \tag{3}$$

Solutions of this system will generally be obtained numerically, for randomly generated sequences of the white noise; these are easily developed on a personal computer with simple discretisation algorithms (see below) and with repetitive multiple realisations for statistical sampling.

Fokker-Planck Equations

The key to this problem is the drift function $\omega(s)$. The standard approach is to use the Fokker-Planck equation corresponding to (1) to constrain the drift term $a(u,l)$ [4]. The implications for $\omega(s)$ are then determined by letting $l \to 0$. According to (1) the Lagrangian transition joint probability density function for *u* and *l*, $P(u,l,t;u_0,l_0,t_0)$, satisfies

$$\frac{\partial P}{\partial t} + u\frac{\partial P}{\partial l} + \frac{\partial aP}{\partial u} = \tfrac{1}{2}\chi^2\frac{\partial^2 P}{\partial u^2} \tag{4}$$

and when averaged over suitable initial conditions [5], (4) yields the Eulerian equation (for non-decaying turbulence)

$$\frac{u}{l^2}\frac{\partial l^2 P_E}{\partial l} + \frac{\partial aP_E}{\partial u} = \tfrac{1}{2}\chi^2\frac{\partial^2 P_E}{\partial u^2}. \tag{5}$$

Finally, in the limit of the dissipation sub-range where $u = sl$, $P_E = \sigma_s^{-1}l^{-1}p_E(s/\sigma_s)$, and $\partial/\partial l \to \partial/\partial l - sl^{-1}\partial/\partial s$, the change of independent variables gives

$$sp_E - s^2\frac{\partial p_E}{\partial s} + \frac{\partial \omega p_E}{\partial s} = \tfrac{1}{2}\chi_0^2\frac{\partial^2 p_E}{\partial s^2}. \tag{6}$$

From (6), for a given p_E, it is a simple matter to obtain

$$\omega(s)p_E = s^2 p_E - 3\int_{-\infty}^{s} s' p_E ds' + \tfrac{1}{2}\chi_0^2\frac{\partial p_E}{\partial s} \tag{7}$$

as an explicit form for the drift function $\omega(s)$.

On the other hand, the Lagrangian strain-rate evolution described by (3) corresponds to the Fokker-Planck equation for the pdf $p(s)$ given as

$$\frac{\partial p}{\partial t} + \frac{\partial(\omega - s^2)p}{\partial s} = \tfrac{1}{2}\chi_0^2\frac{\partial^2 p}{\partial s^2}, \tag{8}$$

which has the long time "equilibrium" solution as $t \to \infty$

$$p_\infty(s) = n\exp\left(2\chi_0^{-2}\int_0(\omega(s') - s'^2)ds'\right), \tag{9}$$

where *n* is a normalisation constant. Note that, in general, $p_\infty(s) \ne p_E(s)$. Thus while the Eulerian mean value for the strain rate is zero, the Lagrangian mean value of strain, $\bar{s}_\infty = \int_{-\infty}^{\infty} sp_\infty(s)ds = \lambda_\infty$ is a non-zero constant. The implication then is that long-time separation growth is exponentially fast,

$$l = l_0\exp\left(\int_0 s(t')dt'\right) \sim l_0\exp(\lambda_\infty t) \quad t \to \infty, \tag{10}$$

and this accords with a common expectation [11], along with $\lambda_\infty > 0$, so that particle pairs eventually always separate.

In summary, the dissipation sub-range behaviour is characterised by exponential growth of the separation, at least for long times and while the separation remains within the dissipation sub-range. More general numerical solutions of (3) will be considered below, for particular forms of the Eulerian strain-rate pdf.

Eulerian Parameterisations

The Eulerian pdf function $p_E(s)$ must be given in order to use the stochastic models as formulated. One convenient way to parameterise this function is to use an exact transport equation [12;13]: if $A = \langle \dot{u}|u,l\rangle \approx \alpha + \beta u + \gamma u^2 \quad (\dot{u} = du/dt)$, then

$$\frac{u}{l^2}\frac{\partial l^2 P_E}{\partial l} = -\frac{\partial AP_E}{\partial u}. \tag{11}$$

Here *A* is the conditional rate of change of the separation rate (it is like an acceleration). The quadratic-form assumption is found to be quite reliable when compared with direct numerical simulations, particularly in the dissipation sub-range [13]. In the strain-rate model limit $A = (\alpha_0 + \beta_0 s + \gamma_0 s^2)l$ and

$$sp_E - s^2\frac{\partial p_E}{\partial s} = -\frac{\partial(\alpha_0 + \beta_0 s + \gamma_0 s^2)p_E}{\partial s} \tag{12}$$

then moments of (12) then yield

$$3\overline{s^n} = (n-1)\left(\alpha_0\overline{s^{n-2}} + \beta_0\overline{s^{n-1}} + (\gamma_0 - 1)\overline{s^n}\right), \quad (n = 2,3,4) \tag{13}$$

which can be solved for the coefficients in the quadratic form to give:

$$\alpha_0 = \sigma_s^2(4-\gamma_0),\ \beta_0 = \sigma_s S\left(\tfrac{5}{2}-\gamma_0\right),\ \gamma_0 = 1+\frac{K-\frac{3}{2}S^2-3}{K-S^2-1} \quad (14)$$

where the skewness is $S = \overline{s^3}/\sigma_s^3$, and the flatness $K = \overline{s^4}/\sigma_s^4$. Thus the first four moments of the strain rate determine the model fully; in fact the complete Eulerian solution of (12) is

$$p_E = \tilde{n}\left(\alpha_0+\beta_0 s+(\gamma_0-1)s^2\right)^{-\phi} \times \exp\left(\frac{3\beta_0 \tan^{-1}\left((\beta_0+2(\gamma_0-1)s)/\Delta\right)}{\Delta(\gamma_0-1)}\right) \quad (15)$$

with $\phi = 1+\frac{3}{2}(\gamma_0-1)^{-1}$, $\Delta = \sqrt{4\alpha_0(\gamma_0-1)-\beta_0^2}$ and $\tilde{n}$ is the normalisation constant so that $\int_{-\infty}^{\infty} p_E\,ds = 1$.

Figure 1 shows solutions for the strain-rate pdf (15) compared with direct simulation data for turbulence with a Taylor-scale Reynolds number of Re_λ = 230, and for the appropriate parameters $S=-0.55, K=10$. The agreement is remarkably good over the range $-5 \le s/\sigma_s \le 5$. The deviations beyond this inner core are crucial for modelling, at least for large positive strains, and this is discussed below.

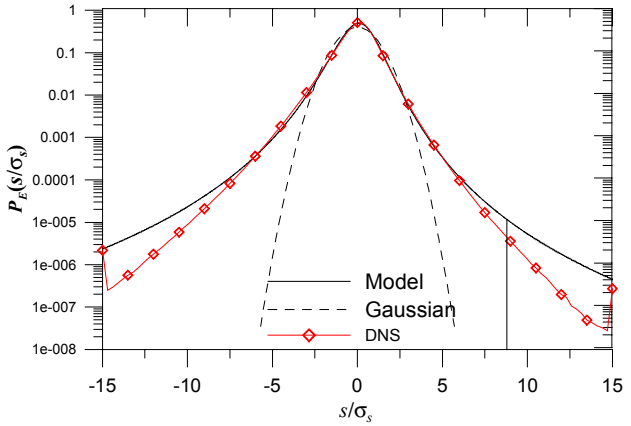

Figure 1. Eulerian pdf for strain rate. Model (15) together with DNS results. Model (15) works well over the inner range but breaks down at larger values. The truncation line shown at s=8.8σ_s is discussed below.

Given (15) we can also easily derive the drift term $\omega(s)$ from (7):

$$\omega(s) = \alpha_0+\beta_0 s+\gamma_0 s^2 - \tfrac{1}{2}\chi_0^2\frac{\beta_0+(2\gamma_0+1)s}{\alpha_0+\beta_0 s+(\gamma_0-1)s^2}, \quad (16)$$

which completes the specification of the stochastic model given just the first few moments of the Eulerian field. However, there is a problem with this solution: the Lagrangian pdf (9) is not well defined over the range $-\infty \le s/\sigma_s \le \infty$, the difficulty evidently is with the infinite upper limit, i.e. for large positive strains. The cubic growth of integrated ω in (9) means that the pdf cannot be normalised over a doubly infinite range of strain. Consequently, we consider the model restricted to the semi-infinite range $-\infty \le s/\sigma_s \le s_\infty/\sigma_s$. For simplicity, the assumption is also made that the upper limit is sufficiently large so that the first few moments are not significantly affected by truncating the tail; thus we do not account for it explicitly in the Eulerian analysis. This avoids an iterative process in the specification of (15) in terms of the moments in (13). According to figure 1 we anticipate that the truncation will be for strain rates $s_\infty/\sigma_s > 5$, which means that only for very high flatness factors will the truncation be a significant factor. The important point to remember is that the main role for the maximum strain-rate truncation is for the Lagrangian growth-rate effects, which is indicated by the sensitivity of (9) to the large strain-rate frequency.

The pdf (15) for large strain is characterised by a *power-law* tail, which is quite "heavy", which is to say the frequency is much greater than Gaussian estimates. Beyond an upper bound, however, the tails of the actual pdf decay faster than any power-law, and stretched exponential models are common in the literature [14]. What this means is that there is always an effective cut-off of the quadratic-form model. Equation (7) shows that, provided p_E decays faster than a power law for large s, $\omega \sim s^2 + o(s^2)$ as $s \to \infty$, in which case the cancellation of the leading order quadratic in (9) permits an equilibrium solution for $p_\infty(s)$. However, for simplicity and numerical convenience, we shall consider a simpler hard-cut-off model where $p_E = 0, s \ge s_\infty$. Thus s_∞ is a lumped parameter representing the effective truncation of the maximum effective strain rate for separation effects in turbulence. A better model of course would use more precise tails for the pdf, but this is excessively complex and the simplicity of a single parameter representing the important effects is sufficient for our purposes.

Numerical Methods

The stochastic model for Lagrangian strain is particularly easy to solve numerically. A simple forward difference of (3) gives

$$s_{n+1} = s_n + \left(\omega(s_n) - s_n^2\right)\Delta t + \chi_0\sqrt{\Delta t}\,\xi_n \quad (17)$$

where ξ_n is an independent Gaussian random variable at each time step with $\overline{\xi_n} = 0$ and $\overline{\xi_n^2} = 1$. The strain at the initial step, s_0, is selected to match the distribution of Eulerian strains according to (15). The time step is assumed to be uniform for our purposes so that $s(n\Delta t) = s_n$ and $\Delta t << t_\eta$. For comparisons with existing turbulence simulations [3,13,15] we calculate for time spans of the order of $10t_\eta$. This is because the simulations that begin with $l_0 = \frac{1}{4}\eta$ evidently retain dominant dissipation range character for the time range suggested, but after this time significant numbers of separations are beyond the dissipation sub-range. For a given realisation of a sequence of Lagrangian strains, say $\{s_i; i = 0,1,2,\cdots,N\}$ the corresponding separation is determined with the trapezoidal rule in (3):

$$\log(l_n/l_0) = \tfrac{1}{2}\Delta t\sum_{i=0}^{n-1}(s_i + s_{i+1}). \quad (18)$$

Statistics are obtained with M = 4x10^5 independent realisations. An ensemble of realisations, say $\{l_n^{(i)}; i = 0,1,2,\cdots,M\}$ at a particular time instant, $t = n\Delta t$, gives the statistics; for example, the mean separation is $\bar{l} = \overline{l_n} = \frac{1}{M}\sum_{i=0}^{M} l_n^{(i)}$. Results are obtained (shown in the next section) for the mean, $\bar{l}$, the root-mean-square σ_l, where $\sigma_l^2 = \overline{l^2}$; and the third- and fourth-order higher moments as the skewness and flatness respectively:

$$S = \overline{(l-\bar{l})^3}\Big/\overline{(l-\bar{l})^2}^{3/2} \text{ and } F = \overline{(l-\bar{l})^4}\Big/\overline{(l-\bar{l})^2}^{2}. \quad (19)$$

The parameters $\chi_0 = 3.15t_\eta^{-3/2}$ and $s_\infty = 8.8\sigma_s$ are selected by fitting the growth of the mean and root-mean-square separation against the direct numerical simulations. The test of the model is to predict the non-Gaussian effects reflected in higher moments. The truncation approximation is illustrated in figure 1.

Results

Figures 2 to 5 show the separation statistics. Compared with direct numerical simulation data the agreement is very good for most times as shown, but there is a systematic deviation as increasingly more pairs leave the dissipation sub-range. The most meaningful comparisons are those for times less than about $3t_\eta$.

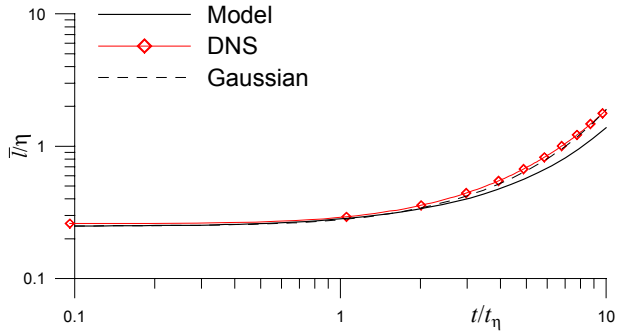

Figure 2. Lagrangian mean separation growth. DNS comparisons from Re_λ=230, l_0/η=0.25. Parameters $\chi_0 = 3.15 t_\eta^{-3/2}$ and $s_\infty = 8.8\sigma_s$.

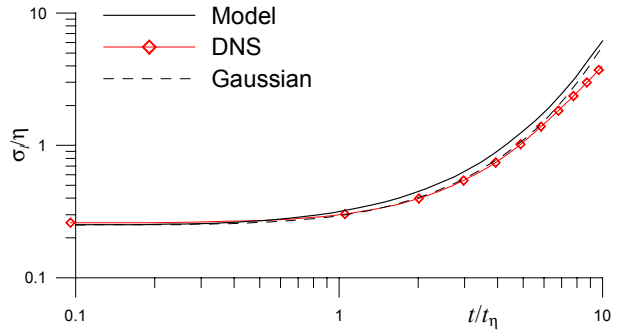

Figure 3. Lagrangian root-mean-square separation growth. DNS comparisons from Re_λ=230, l_0/η=0.25. $\chi_0 = 3.15 t_\eta^{-3/2}$, $s_\infty = 8.8\sigma_s$.

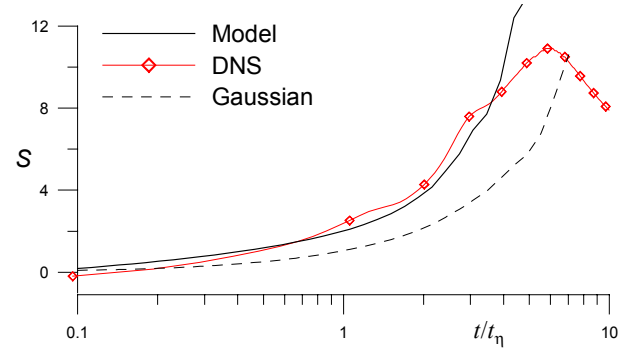

Figure 4. Lagrangian separation skewness as a function of time. DNS comparisons from Re_λ=230, l_0/η=0.25. Note the rapid rise of skewness.

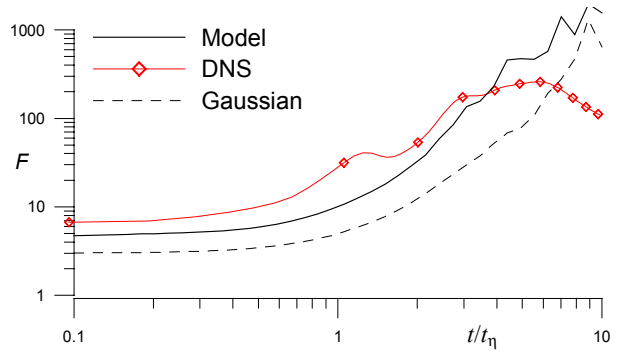

Figure 5. Lagrangian separation flatness as a function of time. DNS comparisons from Re_λ=230, l_0/η=0.25. Note the rapid rise of flatness.

Also shown as dashed lines on figures 2 to 5 are evolutions of separation according to a Gaussian model for p_E, but which typifies results for all models that do not have quadratic-form accelerations and power-law pdf tails for large strains. In those cases it is usual to have numerically much smaller Lagrangian skewness and flatness and also much slower development with time of the strongly non-Gaussian Lagrangian character. Such models essentially have a single parameter χ_0 to tune and are not sensitive to large strain rates. Consequently it is not possible to reasonably match the *rapid* early growth of higher moments as can be seen in figures 4 and 5. Note that, for all models, the growth of the non-Gaussian effects becomes strong at large times because of the exponential separation effect and at which time the separation statistics are trending towards lognormal. However, at such large times the actual simulation behaviour is no longer dissipation sub-range dominated (S and F peak due to inertial range and energy containing scale effects).

Conclusions

The main role of the new model in this paper is to explain the rapid early rise of non-Gaussian effects, not due to accumulated lognormality, but to large strain-rate accelerations. Accordingly, the model is constructed to be sensitive to large strain rates and thus depends on a parameter, s_∞, explicitly reflecting this behaviour. It has been demonstrated at least qualitatively that key characteristics of the pair separation process in turbulence are controlled by the non-Gaussian tails of the Eulerian probability density at large velocities or straining flows. These effects only become evident in Eulerian statistics well beyond five standard deviations and are consequently very rare. Nevertheless, these extreme events largely control even the third or fourth moments of the Lagrangian separation, at least for small times, and the peculiarity of this non-Gaussian behaviour has been noted in the literature. However, both [7] and [8] have wrongly concluded that this highly intermittent extreme behaviour is not reasonably modelled with simple stochastic equations. The point to stress again is that such simple models do allow the representation of the correct physics, provided that the details are specified fully enough. In the context of stochastic models of turbulence, it is also a surprise that important effects lurk well beyond five (Eulerian) standard deviations, and this is an important lesson in general when modelling highly non-linear processes.

References

[1] Richardson, L.F., Atmospheric diffusion shown on a distance-neighbour graph. *Proc. Roy. Soc. London A* **110**, 1926, 709-737.

[2] Sawford, B.L., Turbulent relative dispersion. *Ann. Rev. Fluid Mech*. **33**, 2001, 289-317.

[3] Yeung, P.K., Direct numerical simulation of two-particle relative diffusion in isotropic turbulence. *Phys. Fluids* **6**, 1994, 3416-3428.

[4] Gardiner, C.W., *Handbook of Stochastic Methods for Physics, Chemistry and the Natural Sciences.* 1983. Springer-Verlag.

[5] Thomson, D.J., A stochastic model for the motion of particle pairs in isotropic high-Reynolds-number turbulence, and its application to the problem of concentration variance. *J. Fluid Mech*. **210**, 1990, 113-153.

[6] Kurbanmuradov, O.A., A new Lagrangian model of two-particle relative turbulent dispersion. *Monte Carlo Methods and Appl,*. **1**, 1995, 83-100.

[7] Heppe, B.M.O., Generalised Langevin equations for relative turbulent dispersion. *J. Fluid Mech*. **357**, 1998, 167-198.

[8] Malik, N.A. & Vassilicos, J.C., A Lagrangian model for turbulent dispersion with turbulent-like flow structure: Comparison with direct numerical simulation for two-particle statistics. *Phys. Fluids* **11**, 1999, 1572-1580.

[9] Luhar, A.K. & Britter, R.E., A random walk model for dispersion in inhomogeneous turbulence in a convective boundary layer. *Atmos. Environ.* **23**, 1989, 1911-1924.

[10] Franzese, P., Luhar, A.K. & Borgas, M.S., An efficient Lagrangian stochastic model of vertical dispersion in the convective boundary layer. *Atmos. Envrion*. **33**, 1999, 2337-2345.

[11] Monin, A.S. & Yaglom, A.M., *Statistical Fluid Mechanics.* **Vol II** (J.L. Lumley ed.), 1975, M.I.T. Press, Cambridge, MA.

[12] Pope, S.B., *Turbulent Flows.*, Cambridge University Press. 2000.

[13] Borgas, M.S. & Yeung, P.K., Conditional fluid particle accelerations in turbulence. *Theoret. Comput. Fluid Dynamics* **11**, 1998, 69-93.

[14] Sornette, D., *Critical phenomena in natural sciences: chaos, fractals, self-organisation and disorder: concepts and tools,* 2000. Springer.

[15] Borgas M.S. & Yeung P.K., Modelling relative dispersion in finite Reynolds number turbulence. To be submitted *J. Fluid Mech*. 2001.